

## ANALYSIS OF THE AIRFRAME REPAIR NODE

### ANALIZA WĘZŁA NAPRAWCZEGO POKRYCIA PŁATOWCA

#### Abstract

Polymer composite materials can be used both for the production of semi-monocoque structures and for the repair of aircraft airframes. Of all the elements of the semi-monocoque structure, the airframe skin is most often damaged during operation. The fragments of the skin between the frame elements of the semi-monocoque structure are considered as a thin-walled plate. The paper presents an analysis of the repair node of a metal plate subjected to uniform shear. The model of the repaired plate made in the Ansys Workbench environment was used for the analysis. The boundary conditions were defined by means of an articulated frame using the possibilities of the computing environment in the scope of, defining elements among others. The model was initially verified experimentally, assuming that it can be used to carry out a comparative analysis of two methods of repairing a damaged plate, using CFRP (Carbon Fiber Reinforced Polymer) and GFRP (Glass Fiber Reinforced Polymer) materials. Analyzing the obtained results, it was found that the repair does not restore the original strength of the damaged structure, however, it reduces the stress of the plate material around the opening by 10%.

**Keywords:** numerical analysis, experimental research, repair node, semi-monocoque structure, buckling, Ansys Workbench

#### Streszczenie

Polimerowe materiały kompozytowe mogą być wykorzystywane zarówno do wytwarzania elementów konstrukcji półskorupowych jak i do napraw już eksploatowanych metalowych płatowców statków powietrznych. Spośród wszystkich elementów konstrukcji półskorupowej, pokrycie płatowca ulega najczęściej uszkodzeniom eksploatacyjnym. Fragmenty pokrycia pomiędzy elementami szkieletu konstrukcji półskorupowej rozpatruje się jako płytę cienkościenną. W pracy przeprowadzono analizę węzła naprawczego metalowej płyty poddanej równomiernemu ścinaniu. Do analizy wykorzystano model naprawianej płyty wykonanej w środowisku Ansys Workbench. Warunki brzegowe zdefiniowano za pomocą przegubowej ramki wykorzystując możliwości środowiska obliczeniowego w zakresie m.in. definiowania kontaktów. Model wstępnie zweryfikowano eksperymentalnie, przyjmując założenie, że może być wykorzystywany do przeprowadzenia analizy porównawczej dwóch metod naprawy uszkodzonej płyty, z wykorzystaniem materiałów CFRP (Carbon Fibre Reinforced Plastic) oraz GFRP (Glass Fibre Reinforced Plastic). Analizując otrzymane wyniki stwierdzono, że naprawa nie przywraca pierwotnej wytrzymałości uszkodzonej struktury, jednakże zmniejsza wyężenie materiału płyty wokół otworu o 10%.

**Słowa kluczowe:** analiza numeryczna, badania doświadczalne, węzeł naprawczy, struktura półskorupowa, wyboczenie, Ansys Workbench

## 1. Introduction

The airframes of modern aircrafts are most often semi-monocoque structures [1], which consist of a frame and load-carrying skin [2]. Both the frame and the skin contribute to the load transmission. The share of airframe elements structure in the distribution of loads (bending and torsion) is unequal.

Normal stresses resulting from bending are transferred mainly by the wing spars, stringers and skin, while the shear stress resulting from bending and torsion are loaded by wing spars wall and skin. During the strength analysis, the skin is considered as a thin-walled plate [3]. One of the special features of each thin-walled structure is its low bending stiffness in the

direction perpendicular to the skin plane and its susceptibility to loss of stability and buckling [4, 5].

In the process of operation, the airframe skin is the element that is most often damaged (98 - 100%) [6]. The damage may be a single element damage or a coupled damage (the skin and, additionally, other elements of the aircraft are damaged, e.g. stringers, wing spars, other force elements of the frame) [7,8,9]. These damages are particularly important when they occur in the wing structure, due to its tasks, including the creation of lift, stability and controllability [10]. Damage most often occurs as a result of impact on the structure, e.g. in conditions of improper use. In the case of a military aircraft, additional damage may occur due to the effect of combat measures [6, 11].

<sup>1</sup> dr hab. inż. Marek Rośkowicz, marek.roskowicz@wat.edu.pl, ORCID: 0000-0003-0501-0622.

<sup>2</sup> mgr inż. Iga Barca, iga.barca@wat.edu.pl, ORCID: 0000-0003-4687-4873.

In the process of maintenance, aircraft airframes are repaired. Repairs are carried out in order to restore the original strength of the structure and stop the process of damage development [12, 13]. In aviation, two basic methods of repairing aircraft skin are used: the method with the use of metal patches and mechanical joints [14] and the use of composite patches and adhesive joints [15, 16] or alternatively a hybrid solution [17, 18, 19]. Due to the technological susceptibility of fiber-reinforced composite materials, these types of materials are used to repair not only composite but also metal structures. Polymer composite materials are bonded to the damaged structure with adhesive materials [20, 21].

The purpose of the performed calculations and tests was to assess the effectiveness of repairing a damaged plate, which was subjected to uniform shear. The metal plate was repaired with composite materials. Implementation of works on experimental tests and calculations using the finite element method were performed. Using the finite element method, calculations were carried out on the basis of a metal plate model which was repaired with composite patches.

## 2. Model of plate and frame

In order to perform numerical calculations, a simplified model of the plate with a loading frame was prepared in the NX 11 environment. As part of the model being performed, the plate, repair elements, articulated joints and a frame for mapping the plate shear were defined. The following assumptions were adopted to define the plate model: thickness 1 mm and material properties of the 2024-T3 series aluminum alloy. The geometrical dimensions of the plate with a damage in the form of a hole with a diameter of 50 mm are presented in Fig. 1.

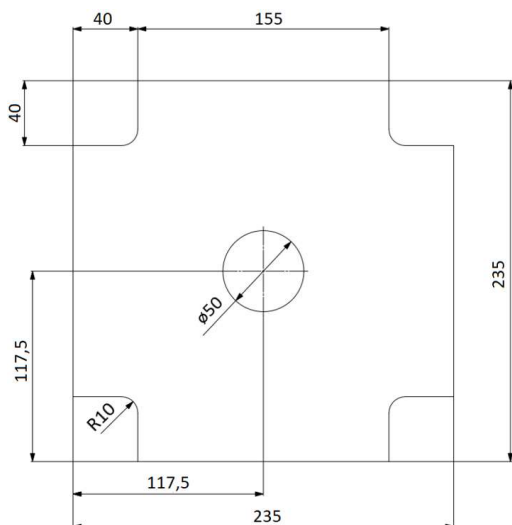


Fig. 1. Dimensions and shape of the plate used in the test

The model of the repaired plate consisted of elements that are used in the repair process. Inside the hole, a metal insert is defined, while on one of the outer surfaces of the plate a composite patch with the material properties of a glass (GFRP) and carbon (CFRP) composite was modeled. The properties of the glass composite corresponded to the material prepared on the basis of SynglassE86 glass fabric with a grammage of 101 g/m<sup>2</sup> and the L285/H285 (MGS) impregnated by Havel Composites (Fig. 2).

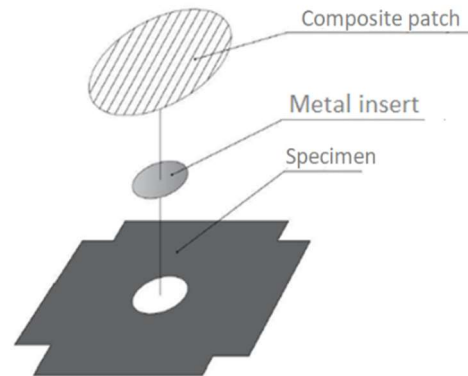


Fig. 2. Elements of the repair node

The properties of the carbon composite were defined on the basis of 160 g/m<sup>2</sup> carbon fabric by HACOTECH and L285/H285 (MGS) by Havel Composites. The composite patch had the shape of a clipped cone with a back diameter of 142 mm and a top layer diameter of 127 mm (Fig. 3). Due to the use of a conical shape, the occurrence of stress concentration in the joint of the adhesive joint at the edges of the edge overlap was limited. Between the patch and the panel to be repaired, an adhesive layer was modeled with a thickness of 0.1 mm, diameter of 142 mm and the properties of Epidian 57/Z1 adhesive [22].

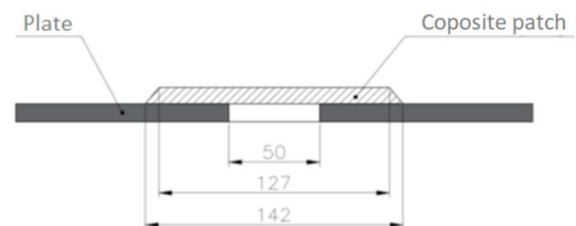


Fig. 3. The diagram of the repair node

As part of defining the boundary conditions in the load area, a model of the mounting frame was made, which consists of eight steel flat elements connected with each other articulated with four pivots. The scheme of the frame with the plate being repaired is shown in Fig. 4.

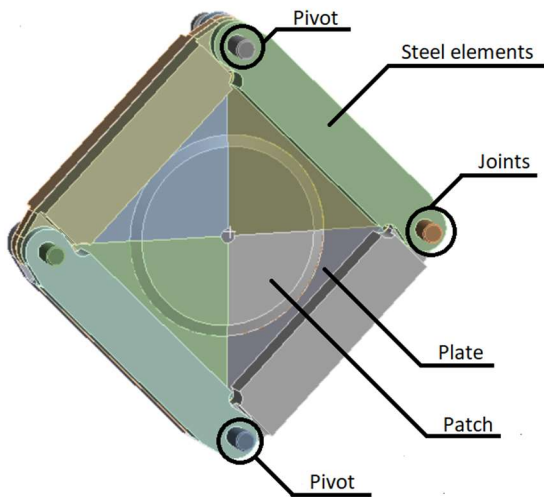


Fig. 4. Geometric model of the repaired plate with a frame

The plate geometries with the frame were exported to the Ansys Workbench 21 R2 environment for numerical calculations. For the preparation of the calculation model, the material properties of individual elements were defined. Epidian 57 adhesive parameters were adopted from the publication [22]. As part of solving the task, a simplification assuming quasi-isotropic properties of composite materials was adopted. Properties of the materials defined in the model are presented in Table 1.

Table 1. Properties of materials defined for calculations

| Material                | Young's module [MPa] | Poisson number |
|-------------------------|----------------------|----------------|
| Aluminium alloy 2024-T3 | 73100                | 0,33           |
| Adhesive Epidian 57/Z1  | 2083                 | 0,35           |
| Glass composite (GFRP)  | 40000                | 0,4            |
| Carbon composite (CFRP) | 61340                | 0,3            |
| Steel elements - Steel  | 200000               | 0,3            |

Using the symmetrical layout of the plate, a regular shape of the plate mesh was defined. For this purpose, the board model was divided into 8 elements (Fig. 5). This type of operation was aimed at obtaining a mesh with a regular shape - Fig. 6.

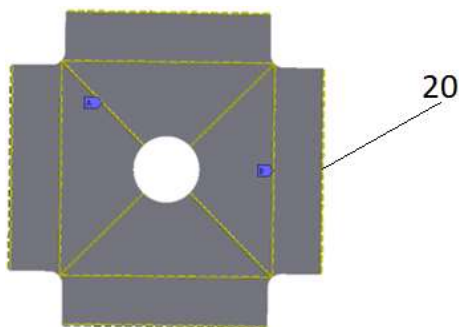


Fig. 5. Scheme of division of the slab model into 8 geometric elements

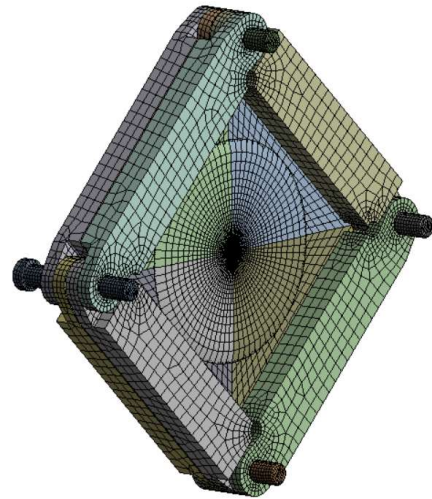


Fig. 6. The view of the model with the division into finite elements, the so-called mesh

The Edge Sizing option was used to define the mesh, assigning 20 elements to individual edges, and the MultiZone option, assuming the type of Hexa element. According to the adopted scheme, a similar division of the composite patch, the adhesive layer and the insert was made. Additionally, the frame elements have been assigned an optimization module of the Hex Dominant type. As a result of discretization, the frame model had 53362 finite elements and 62506 mesh nodes, while the repaired plate had 2400 elements and 5000 nodes.

### 3. Defining contact elements

In order to recreate the conditions of assembly the plate to the frame, bonded contacts have been defined between the frame and the plate. The same type of contact is defined between the composite patch and the adhesive layer and between the adhesive layer and the plate and between the insert and the adhesive layer. Figure 7 shows the individual elements for which the type of bonded contact has been defined.

The articulated joints were modeled between the frame elements and the pivots using a No Separation contact (slip without friction, Fig. 8).

The last type of contact that was used in the modeling of the plate with the frame was the Frictional contact, which was assigned to the side surfaces of the insert and the hole. For the purposes of the analysis, the friction coefficient of 0.1 was assumed.

In the load area, a force of 8 kN was defined located in the pivot No. 1 directed along the z axis, while the pivot No. 4 was fixed using the Fixed Support function (Fig. 9).

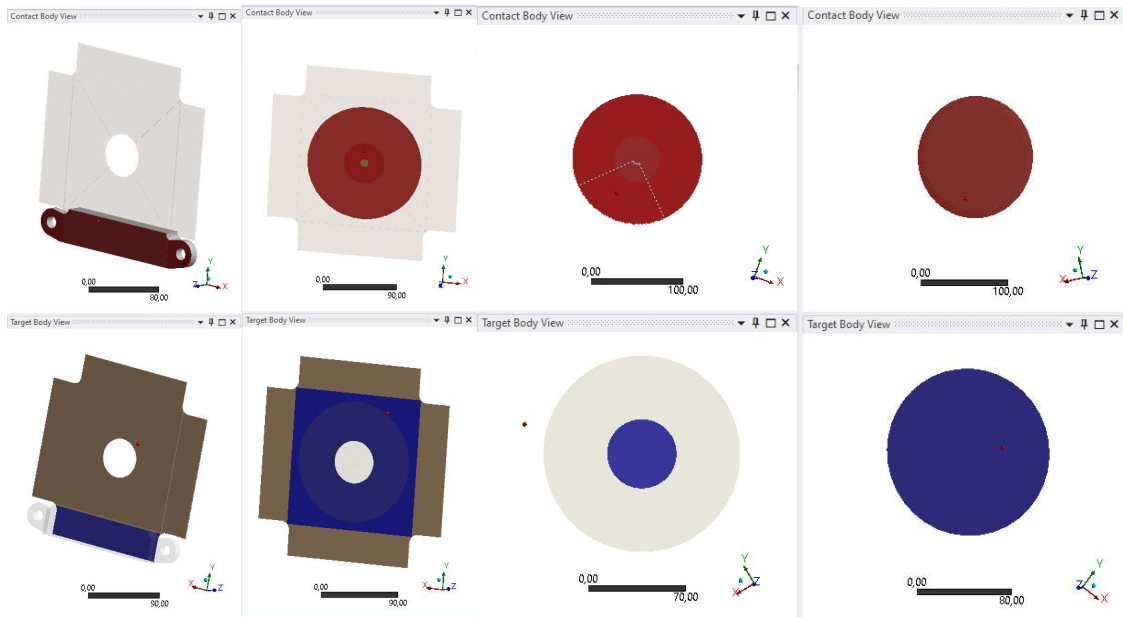


Fig. 7. Bonded contacts between the individual elements (red and purple indicate the contact area), from the left, the frame with the plate, the adhesive layer with the plate, the adhesive layer with the insert and the adhesive layer with the patch



Fig. 8. View of elements between which a No Separation type connection has been defined

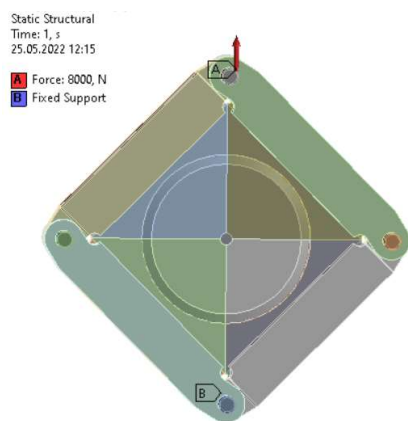


Fig. 9. The diagram of the boundary conditions of the FEM model

## 4. Experimental verification of the model

In order to made assess the quality of the model, calculations were carried out under the conditions of the planned experiment (8 kN load). The obtained results, in regard to of strain, were compared with the results of experimental tests.

### 4.1. Experimental tests of the plate

The specimen for experimental tests was made of 1 mm thick 2024-T3 sheet, aluminium alloy with the dimensions shown in Fig. 1. The repair of the plate consisted of installing a metal insert in a hole with a diameter of 50 mm. The composite patch was formed of 16 layers of SynglassE86 glass fabric with diameters from 127 mm to 142 mm, in 1 mm increments. The test surface was degreased with extraction naphtha and with the use of a 3M SC-DR disc of granularity P180 and P400. Only the area on which the patch was to be formed was processed. The surface preparation process was completed with another surface cleaning with extraction naphtha. The L285 epoxy resin mixed with the H285 hardener in the proportions 100: 40 was used as the saturant of the composite patch. The filtered material layers were layered according to the scheme  $[0^\circ, 30^\circ, 60^\circ, 90^\circ]_4$ . Then, next layers used in the vacuum bag technology, including a resin draining mat, perforated foil and delaminating fabric, were applied to the composite patch. The patch prepared in this way was placed in a device enabling to generate a pressure equivalent to a pressure of 0.8 MPa and left for 24 h at room temperature (according to the technical sheet for curing resin L285/H285). The prepared composite patch was adhesively bonded to

the plate with the use of Epidian 57 epoxy resin mixed with the hardener Z1, in a ratio of 1:10. The adhesive has been hardened: in the first stage, 24 hours at 20°C and for 6 hours at 80°C.

After the specimen was prepared, mounting holes were drilled in it and the specimen with the frame was placed in the traverses of the testing machine. The specimen and the method of its mounting in the machine are shown in fig. 10.

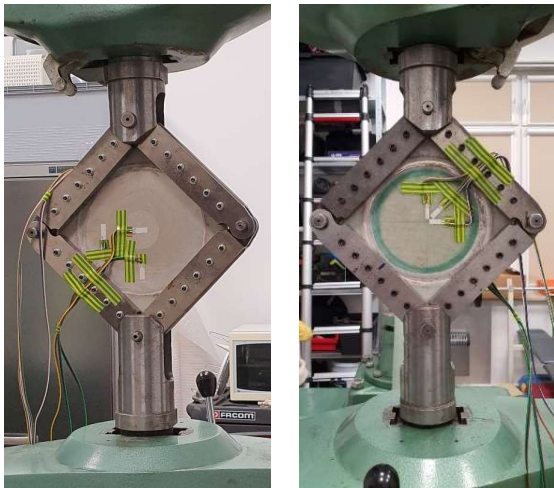


Fig. 10. Fixing the sample in the testing machine

Strain gauges were jointed to the elements of the repair node in accordance with the diagram shown in Fig. 11.

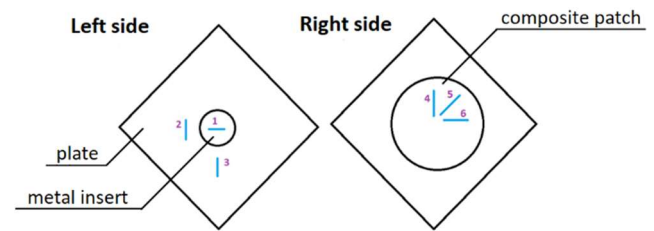


Fig. 11. Distribution and numbering of strain gauges mounted on the specimen

The strain gauge No. 1 is jointed to the metal insert - in the direction perpendicular to the load generated by the testing machine. Strain gauges 2 and 3 were jointed in the direction of load deformation of the testing machine. The strain gauges 4, 5, 6 had the form of a rosette bonded to the composite patch. A CL 460 (Zakład Elektroniki Pomiarowej Wielkości Nielektrycznych, Poland) bridge was used to measure the deformation.

The results of the recorded strain from the experimental tests were compared with the results of the numerical simulation (Fig. 12 and Table 2).

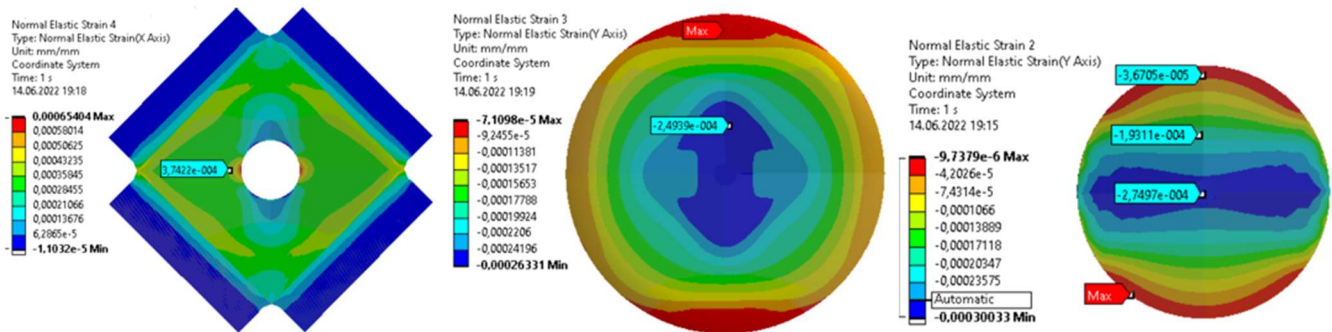


Fig. 12. Deformation values for the plate, glass fiber patch and reinforcement insert

Table 2. Values of deformations obtained in the experimental test and numerical simulation

|                     | Canal 1   | Canal 2  | Canal 3  | Canal 4 | Canal 5   | Canal 6   |
|---------------------|-----------|----------|----------|---------|-----------|-----------|
|                     | m/m       | m/m      | m/m      | m/m     | m/m       | m/m       |
| <b>Experiment</b>   | -0,000465 | 0,000685 | 0,000598 | 0,00098 | -0,000081 | -0,000545 |
| <b>Calculations</b> | -0,000300 | 0,000654 | 0,000654 | 0,00035 | -0,000050 | -0,000260 |

The largest differences in strain between the results of the experimental tests and the results of calculations occur on the composite patch, which may be related to the take simplifications in defining the composite material. In the case of strain gauges

bonded directly to a metal plate, the differences are at the level of several percent. Therefore, it was assumed that the prepared model can be used for further analyzes.

## 5. Calculations of the repairing plate

In order to compare the effectiveness of the plate repair with different composite materials (CFRP and GFRP), calculations were carried out using the prepared model. Under boundary conditions, the load values were changed from 8 kN to 25 kN. According to the results presented in [23], it was the range of subcritical loads in buckling process of plate. Computational simulations were carried out for the undamaged, damaged and repaired plate model. Examples of calculation results in the form of reduced stresses (von-Mises) for an undamaged and damaged plate are presented in Fig. 13.

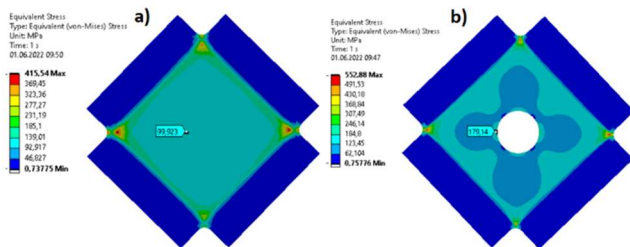


Fig. 13. Reduced stresses in the plate for undamaged (a) and damaged (b)

Stress concentration in an undamaged plate occurs near the corners of the plate. Which in the conditions of a semi-monocoque structure may cause additional stress on the mechanical joints. In the central zone of the plate, where the stress wave formation process takes place, the stress values are below the yield point. Figure 14 presents the results of the stress distribution in the plate repaired with composite patch in two variants (option I - glass composite GFRP, option II - carbon composite CFRP).

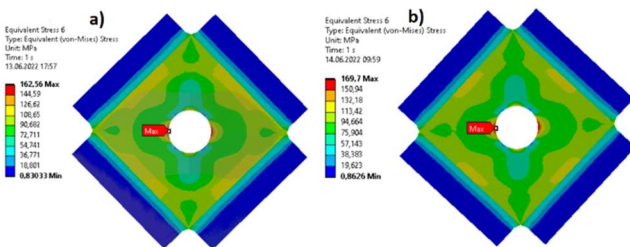


Fig. 14. Reduced stresses in the plate with the GFRP (a) and CFRP (b) patch

Using both GFRP and CFRP, the effort conditions of the undamaged plate were recreated. The greatest changes were observed in the area of the insert mounting hole. The comparison of normal stresses perpendicular to the adhesive surface and the maximum main stresses in the adhesive layer for two patch variants is shown in Fig. 15 and Fig. 16.

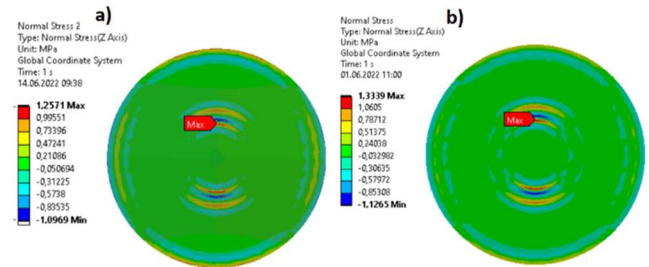


Fig. 15. Normal stresses to the adhesive surface for two patch variants: GFRP (a), CFRP (b)

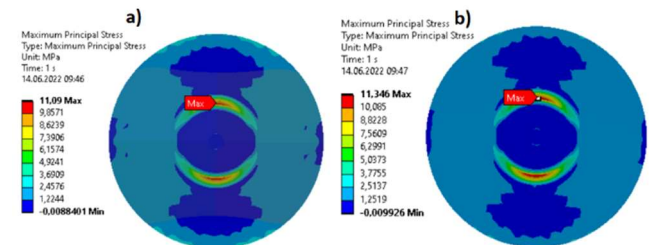


Fig. 16. Maximum main stresses in the adhesive layer for two patch variants: GFRP (a), CFRP (b)

The values of stresses in the adhesive joint area are lower than the values of breaking stresses defined for Epidian 57/Z2. Table 3 presents the displacement values of the frame model with the specimen for the considered repair values. The smallest values occurred for the CFRP composite patch.

Table 3. Displacement values of the frame with the plate for the considered cases

| The type of the plate                          | Plate without damage | Plate with damage | Plate – glass patch | Plate – carbon patch |
|--|----------------------|-------------------|---------------------|----------------------|
| Displacement in the direction of the load [mm] | 0,38                 | 0,43              | 0,248               | 0,25                 |

## 6. Conclusions

Based on the calculations and experimental tests performed, the following conclusions can be defined:

- the aircraft skin repair node, in which composite materials are used, can locally "stiffen" a part of the semi-monocoque structure. The consequence of repairing the skin located between the frame elements of the semi-monocoque structure may be a greater effort of the mechanical joints located in the vicinity of the repaired area.
- repair does not restore the original strength of the damaged structure, however, it reduces the strain of the plate material around the opening by about 10%.
- regardless of the taken variant of the composite patch (GFRP, CFRP), the effectiveness of the repair should be confirmed in experimental tests (especially with the use of the CFRP patch - low susceptibility to deformation of carbon fibers in the process of plate buckling may cause an unfavorable phenomenon of peeling off of the composite patch.
- it seems that in order to evaluate the adopted solutions more effectively, the composite patch for calculations should be defined as layered materials - (the homogenization of the material properties of the composite patch adopted for calculations may negatively affect the stress distribution in the adhesive layer.

## Bibliography

1. Beukers A., Bersee H., Koussios S., Future "Aircraft Structures: From Metal to Composite Structures". Springer. 2011.
2. Standridge Michael., "Aerospace materials — past, present, and future". Aerospace Manufacturing and Design. 2014.
3. Cichosz Edmund, Kierkowski Jerzy, „Przybliżone obliczenia wytrzymałościowe płatowca”. WAT. Warszawa 1968.
4. Bałon P., Świątoniowski A., Rejman E., Kiełbasa B., Smusz R., Szostak J., Kowalski Ł., Bałon N., Cieślak J., „Zastosowanie cienkościennych konstrukcji integralnych w lotnictwie na przykładzie SAT-AM”. Zeszyty naukowe Politechniki Rzeszowskiej 300, Mechanika 92 RUTMech, t. XXXVII, z. 92 (2020), s. 5-17.
5. Zerbst U., Heinemann M., Donne C.D., Steglich D., "Fracture and damage mechanics modelling of thin-walled structures – An overview". Engineering Fracture Mechanics 76 (2009) 5-43.
6. Godzimirski J., „Naprawa płatowców”. WAW. Warszawa 1998.
7. Tavares S.M.O., de Castro P.M.S.T., "An overview of fatigue in aircraft structures". Fatigue & Fracture of Engineering Materials & Structures. 2017.
8. Jones A., Peel C.J., "The analysis of aircraft component failures". In: Goel V.S. editor. Analysing failures: the problems and the solutions. Cleveland, OH: American Society for Metals, 1986.
9. Jones R., Chiu W.K., Smith R., "Airworthiness of composite repairs: failure mechanisms". Engineering Failure Analysis. 1995: 2: 117-128.
10. Galiński C., „Wybrane zagadnienia projektowania samolotów”. Biblioteka Instytutu Lotnictwa, Warszawa 2016.
11. Lewitowicz J., „Podstawy eksploatacji statków powietrznych, cz. 4”. Wydawnictwo ITWL, Warszawa 2007.
12. Goranson Ulf G., "Fatigue issues in aircraft maintenance and repairs". Elsevier. Boeing Commercial Airplane Group, Seattle, WA, USA. 2017.
13. Bouiadja B.B., Benyahia F., Albedah A., Bouiadja B.A.B., "Comparison between composite and metallic patches for repairing aircraft structures of aluminium alloy 7075 T6". International Journal of Fatigue 80 (2015), 128-135.
14. Kedward K., Kim H., "Joining and Repair of Composite Structures". ASTM Stock Number: STP1455, International, USA, 2005.
15. Katnam K.B., Da Silva L.F.M., Young T.M., "Bonded repair of composite aircraft structures: A review of scientific challenges and opportunities". Progress in Aerospace Sciences 61 (2013) 26-42.
16. Baker A., Chalkley P., "Development of a generic repair joint for certification of bonded composite repairs". International Journal of Adhesion and Adhesives, vol. 19, 1999.
17. Romilly D.P., Clark R.J., "Elastic analysis of hybrid bonded joints and bonded composite repairs". Composite Structures Volume 82, Issue 4, 2008, Pages 563-576.
18. Chang P., Heller M., Wang J., Opie M., Yu X., "A New Approach for Hybrid Bonded Repair of Metallic Components" Journal article in preparation, 2017.
19. Wang J., Baker A., Chang P., "Hybrid approaches for aircraft primary structure repairs" Composite Structures, 2018.
20. Chester R., Chapter 2 Materials Selection and Engineering. "Advances on the Bonded Composite Repair of Metallic Aircraft Structure", vol. 1, pp. 19-40. Australia 2002.
21. Baker A., Chester R., Mazza J., "Bonded Repair Technology for Aging Aircraft". Defence Technical Information Center, Compilation Part Notice ADP014082. 2001.
22. Godzimirski J., Tkaczuk S., "Numerical calculations of adhesive joints subjected to shearing". Journal of Theoretical and Applied Mechanics. 45, 2 pp. 311-324, Warsaw 2007.
23. Rośkowicz M., Tkaczuk S., „Połączenia adhezyjne w naprawach pokryć płatowców”. Technologia i Automatykacja Montażu. 3/2010, pp. 32-35.

This work was financed by Military University of Technology under research project UGB 779/2022.